



Studies on decolorization of dye wastewater in down flow jet loop sparged reactor using response surface methodology

G. Mugaishudeen*, M.S. Shiran, H. Mohamed Mubeen

Department of Chemical Engineering, Kongu Engineering College, Erode – 638 060, Tamil Nadu, India, emails: mugais.chem@kongu.edu (G. Mugaishudeen), msshiran96@gmail.com (M.S. Shiran), md.mubeen0802@gmail.com (H. Mohamed Mubeen)

Received 13 November 2021; Accepted 6 July 2022

ABSTRACT

Textile industries consume large quantities of water during the dyeing process, some amount of dyes remains unfixed and generates colored effluent. Untreated textile wastewater when discharged into the environment is one of the most hazardous practices. Many treatment methods like coagulation–flocculation, adsorption on activated carbon, membrane filtration process, electro-chemical and thermal separation processes are currently in use to treat textile wastewater are not only expensive but also inability to reuse the spent inorganic salts because of color acquired during the dyeing process. The main scope of this study is to propose an alternate method for the decolorization of textile wastewater using a down flow jet loop sparged reactor. Ozone and effluent were entered as gas and liquid phases respectively in a jet loop reactor to treat simulated dye wastewater. Color removal efficiencies have been studied for 100 and 50 ppm of Congo red synthetic dye. Response surface methodology (RSM) was used to optimize the performance of the down flow jet loop sparged reactor. The effect of three variables (effluent flow rate, ozonation time, and the sparger openings) on the percentage of decolorization was evaluated. The optimum condition was found at 0.4 L/min of effluent flow rate, 30 min of ozonation time, and 4 opening spargers for the maximum percentage of decolorization of about 95%–99%. The significance of the RSM model was determined by the R^2 value (95%). The experimental results were in close agreement with model prediction.

Keywords: Down flow jet loop reactor; Decolorization percentage; Dye wastewater; Ozonation; Response surface methodology

1. Introduction

Water is a precious source on earth and its demand is increasing day by day. A recent report says that, by the year 2050, about 5.7 billion people living could be scarce of water for at least a month in a year. And by 2040, the water demand will increase by 50%. About 97% of the world's water resources are salty and less than 1% is potable. The freshwater consumed by the textile industries is also increasing day by day to cater to the current demand in the textile market. For that reason, numerous parts of people suffer from a freshwater deficiency. The textile

industry is responsible for an extensive list of environmental impacts. Dye manufacturing, textile processing, and finishing are very common industries, which generate a huge amount of wastewater. The composition of the textile processing industry wastewater containing dyes, fixing agents, and dyeing auxiliary chemicals is deep in color and highly toxic. Dye is a substance that is used to change the color of the fabric material and is in different forms such as powder, granules, beads, and pastes. In general, dyes are classified into natural and synthetic dyes. Since synthetic dyes are produced more easily than natural dyes, it is more widely used. Synthetic dyes are classified into many different groups according to their chemical structure, for

* Corresponding author.

example, azo, anthraquinone, sulfur, phthalocyanine, and triarylmethane, and they are also classified into different types according to their mode of application for example, direct, disperse, basic, and vat dyeing. The dye effluents are high in color, chemical oxygen demand (COD), biochemical oxygen demand (BOD), pH, and suspended solids [1]. Methylene blue is a cationic azo dye that is widely applied in chemistry, biology, dyeing, and the medical science industry [2]. Methylene blue, Long-term exposure to this dye leads to vomiting, anemia, nausea, and hypertension [3]. Basic violet 16 is a highly soluble, non-volatile cationic azo dye. If consumed by animals or humans, it can cause allergies, skin and eye reactions, gastroenteritis, respiratory, and nervous system problems. Congo red dye comes under the category of azo dye. The azo dyes are hardly degraded due to their properties such as complex molecular structure, high chromaticity, low biodegradability, and high chemical stability [4]. In textile industries there are various types of dyes are used to color the fabrics. Mostly the synthetic dyes are manufactured from petrochemicals.

The textile industry is one of the reasons and responsible for adverse environmental effects. The major destruction caused by the textile industry to the environment is due to the discharge of effluents into the water bodies without treating them and unused solid wastes stored in their backyard. Effluents normally constitute more than 80% of the total secretions released by the industry [5]. The effluents have a high quantity of BOD, COD, color, and inorganic salts. The textile dyes along with a huge quantity of inorganic salts like sodium chloride and sodium sulphate are highly harmful and dangerous which leads to environmental degradation, particularly groundwater pollution. The processing of textile effluents from heterogeneous sources thus offers a huge challenge. Over the years, chemical coagulation along with an activated sludge process was effectively employed to treat textile wastewater. The coagulation and flocculation process produces large amounts of sludge but leads to environmental problems [6]. With the current technology of using reverse osmosis (RO) and thermal evaporation in the textile industry, many technical difficulties are encountered in practice. Difficulties in the operation and maintenance of evaporators include corrosion and scaling problems leading to increased power consumption and reduced efficiency [7]. Production of mixed salt from evaporators containing color, organics, and hardness leads to a lack of reusability. Almost all effluent treatment plants (ETP) are saddled with mountains of salt cake which are difficult to dispose of and the probability of getting leached during the rainy season is very high.

Despite a lot of investigations being carried out in the area of adsorption in recent days, adsorption by activated carbon is an expensive and complicated process [8–10]. An ozone technique especially in the removal of color and COD was found to be an effective alternative. Ozone is a tremendously strong oxidant and the same can disintegrate in an aqueous solution. In some existing and economical industrial applications, it has been trusted as an effective disinfectant and a chemical oxidizing agent. The distinct color is estimated on the original sample without the rehabilitation of suspended solids [11–13]. To overcome the current hurdles in the treatment and reuse

of textile wastewater, we have developed a novel down-flow jet loop reactor with a sparger. Ozone and effluent were considered as gas and liquid phases respectively in jet loop reactor to treat simulated dye wastewater [14–16]. There are certain reactors like photoreactors, glass reactors, and jet loop reactors that have already been used by some researchers to study the decolorization of dye wastewater. In this study, we have used a down flow jet loop sparged reactor for the first time to study the decolorization of dye wastewater. The decolorization percentage of the simulated dye wastewater is evaluated for various effluent flow rates, ozonation time, and the number of sparger openings by using response surface methodology (RSM).

RSM is a mathematical and statistical method used for determining the approximation and optimization of stoichiometric models [6]. RSM has advantages in determining the optimum conditions, lesser number of trials, and the correlation relating the response and independent variables [17]. In this method, the effects of independent variables on the response are analysed, for which central composite design (CCD) or Box–Behnken design (BBD) is widely used [18,19]. In our study, the design experiments are accomplished by BBD and estimated by RSM [20]. BBD relates the linear, quadratic, and interaction effects, and also it requires a minimum number of runs than CCD. The power of RSM is that it gives the maximum amount of information from the minimum amount of work [21].

2. Materials and methods

2.1. Experimental setup

Fig. 1 shows the experimental setup. The apparatus is made of an acrylic column of 4.3 cm diameter and 19 cm length. The jet loop reactor consists of two sections, the top straight throat ejector and the middle cylindrical reactor section. The ejector is nothing but a copper pipe of 15 cm in length with air entry on top whereas water enters tangentially. The reactor comprises a vertical perspex tube with a hemispherical bottom.

The effectiveness of the down flow jet loop reactor significantly relies on the configuration of the sparger. It has

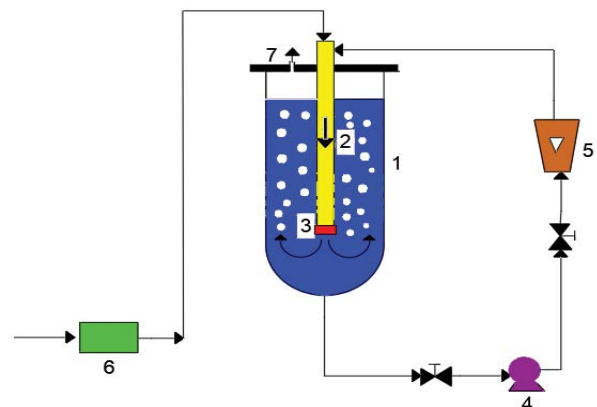


Fig. 1. Schematic representation of the down flow jet loop reactor; 1. Reactor; 2. Straight throat ejector; 3. Sparger; 4. Peristaltic pump; 5. Liquid flow meter; 6. Ozonator; 7. Gas vent.

a significant influence on the dispersion of gas in the liquid phase by creating resistance to the flow and thereby increasing the velocity. The sparger of varying openings and layouts used in our study are shown in Fig. 2. The sparger opening diameter is about 1 mm. The sparger is introduced at the end of the straight throat ejector. The ozone and the effluent phases enter at the top of the straight throat ejector and flow co-currently towards the bottom. The sparger disperses the ozone in the effluent phase leading to bubble formation. The bubbles due to their high velocity imparted from the motive fluid effluent and reach the top of the reactor. This forms an internal loop within the reactor.

The liquid is withdrawn at the bottom of the reactor with the help of a peristaltic pump and recycled back to the straight throat ejector through a liquid flow meter. This forms the external loop. The ozone is sent to the top of the reactor through a gas flow meter by the compact ozonator. The dimensions of the experimental setup are tabulated in Table 1.

2.2. Preparation of Congo red dye solution

Congo red dye was purchased from Global Scientific Company located in Erode, Tamil Nadu, India. The properties of Congo red dye are tabulated in Table 2. Congo red is an asymmetrical azo dye that has been used widely in textile industries for fabric dyeing. The simulated wastewater was prepared by dissolving 50 mg of Congo red dye in 1 L of distilled water to make a concentration of 50 ppm. The λ_{\max} value of Congo red dye is about 499 nm

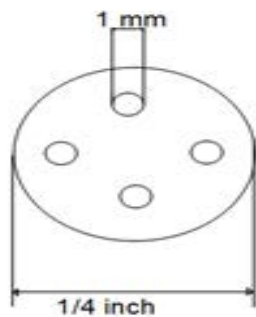


Fig. 2. Perforated sparger opening for 4 openings.

Table 1
Dimensions of down flow jet loop sparged reactor

Parameters	Values
Reactor diameter, cm	4.3
Reactor length, cm	19
Volume of the reactor, mL	308
Length of the ejector, cm	15
Pump capacity, L/min	1–3
Ozone capacity, mg/h	400
Sparger openings	2,3,4
Sparger diameter, mm	1

and for the decolorization studies, λ_{\max} is used for finding the absorbance value.

2.3. Methods

The ozone and the effluent phases enter at the top of the straight throat ejector and flow co-currently towards the bottom as shown in Fig. 1. The ozone flow rate is kept constant throughout the experiment [7]. The ozone is generated by the ozonator (Model: G-35, Greenway) and it has a capacity of 400 mg/h. The ozone dosage time is varied as 10, 20, and 30 min with respect to the effluent flow rate and the number of sparger openings. The liquid flow rotameter has a capacity of 1 L/min and the effluent flow rate is varied as 0.2, 0.3, and 0.4 L/min. The experiment is conducted at room temperature (28°C–31°C) by varying effluent flow rate (0.2–0.4 L/min), ozonation time (10–30 min), and the number of sparger openings (2–4 openings). The color value of the dye solution is estimated by Ultraviolet Spectrophotometer (Model: 119, SYSTRONICS). And measurement is attained at the wavelength of 499 nm. The calibration curve was plotted between absorbance and concentration of known samples as shown in Fig. 3. From this calibration plot, the absorbance values of unknown concentrated solutions are easily determined.

The decolorization of simulated wastewater is determined by:

$$\text{Decolorization}(\%) = \frac{A_0 - A_t}{A_0} \times 100 \quad (1)$$

where A_0 is the initial absorbance value; A_t is the absorbance at the time t .

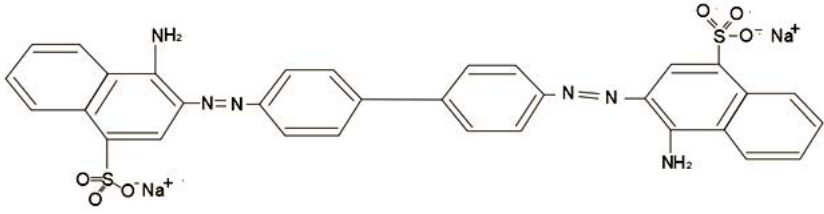
2.4. Response surface methodology

In this work, RSM using Box–Behnken design (Design-Expert version 8) is used to determine the decolorization percentage. RSM is a software whose basic idea is fundamental statistics and mathematical techniques. For the development of empirical formula and the analysis of the data which is influenced by one or more variables, RSM is very useful. Because of the above reasons, several chemical and biochemical industries use RSM. In RSM, the response is the performance response that is affected by one or multiple input variables. RSM reduces the experimental effort while designing the experiments by optimizing the response (output variables) which is affected by the independent variables (input variables). A second-order polynomial response equation is used to correlate the response and independent variables.

CCD is an experimental design used in RSM for building the quadratic model. CCD may be a two-level full factorial or fractional factorial design with included center points and the axial focus moreover known as star points. Whereas the center point is included at the center, the axial points are connected at the center of the levels of a factor for each level of the other factors.

BBD in the RSM is extraordinarily outlined to fit a second-order model, which is very important in most RSM studies. To fit a second-order regression model (quadratic

Table 2
Characteristics of Congo red dye

Molecular formula	$C_{32}H_{22}N_6Na_2O_6S_2$
Molecular weight	696.7 g/mol
Structure	
IUPAC name	Disodium;4-amino-3-[[4-[4-[(1-amino-4-sulfonatophthalen-2-yl)diazenyl]phenyl]phenyl]diazenyl]naphthalene-1-sulfonate
Appearance	Brownish red
Odour	Odourless
Density	0.995 g/mL at 25°C
Melting point	>360°C

model), the BBD as it were needs three levels for each factor, instead of five levels in CCD. The BBD set an intermittent level between the original low- and high-level of factors, maintaining a strategic distance from the extreme axial points as within the CCD. In addition, the BBD uses face points, regularly more practical, instead of the corner points in CCD. The expansion of the mid-level point permits the effective estimation of the coefficients of a second-order model. Moreover, the BBD requires a lesser number of experimental runs as compared with CCD. In the BBD model, the treatment combinations are using the mid-levels of the other factors. Therefore the study is conducted around the expected optimum conditions for all most all experimental values.

$$Y = a_0 + \sum_{i=1}^n a_i p_i + \sum_{i=1}^n a_{ii} p_i^2 + \sum_{j>1}^n \sum_{i=1}^n a_{ij} p_i p_j \quad (2)$$

where Y is the response, p_i and p_j are the coded values of independent variables i and j respectively, a_0 is the constant, a_i is the variable influence on the response (regression coefficient for direct effect), a_{ij} is the interaction effect between i and j (regression coefficient for interplay effect) and a_{ii} is the parameter which defines the curve shape (regression

coefficient for the quadratic effect). The R^2 , F -test, and the coefficient of the determinant are used for the estimation of the polynomial model.

In RSM, the design which is considered to be the best alternative for CCD and also considered as an effective option is the BBD. They require minimum runs to predict higher-order responses. Therefore, it permits the building of sequential design, use of blocks, estimation of parameters of the quadratic model, and determination of the lack of fit of the model. BBD is a round outline with all the focus lying on the sphere of radius $\sqrt{2}$ and also it does not have any points on the vertices of the cubic region for every factor of the upper and lower limits. The second-order polynomial tells the link between response and independent variable. The levels of a factor in this study were chosen as p_1 , p_2 , and p_3 and were described into three coded levels as -1 , 0 , and 1 for lower, middle, and upper respectively as shown in Table 3.

In this study, three independent variables with three levels of BBD have been used for the investigation. $N = 2n(n-1) + N_c$ is the equation used for determining the number of experimental runs, where N_c is the number of central points and n is the number of factors. In this study, $n = 3$ and $N_c = 5$ therefore a total of 17 experiments has to be conducted for 100 and 50 ppm concentration of Congo dye solution. Table 4 shows the BBD matrix for the coded values for different parameter configurations.

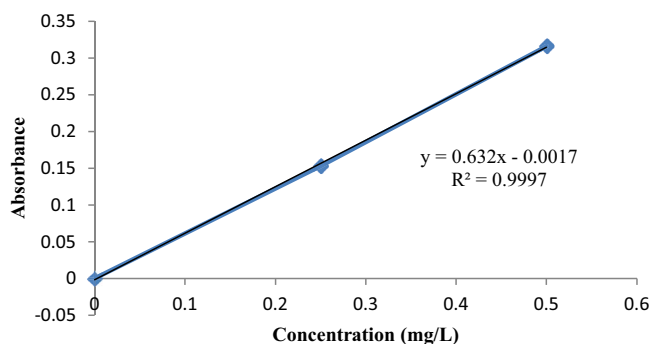


Fig. 3. Absorbance vs. concentration.

Table 3
Experimental and coded values of independent variables

Independent variables	Coded units	Coded levels		
		-1	0	1
Effluent flow rate, L/min	p_1	0.2	0.3	0.4
Ozonation time, min	p_2	10	20	30
Sparger openings	p_3	2	3	4

Table 4
BBD matrix of percentage of decolorization for different reactor configurations

Run order	Decolorization %					
	100 ppm concentration			50 ppm concentration		
	p_1	p_2	p_3	p_1	p_2	p_3
1	0	0	0	0	0	0
2	0	0	0	-1	0	-1
3	0	1	1	0	0	0
4	0	-1	-1	-1	-1	0
5	-1	0	1	-1	1	0
6	0	0	0	0	-1	1
7	-1	-1	0	1	0	1
8	-1	0	-1	1	1	0
9	0	1	-1	0	0	0
10	1	0	-1	1	-1	0
11	1	1	0	0	1	1
12	0	-1	1	0	0	0
13	-1	1	0	0	1	-1
14	1	-1	0	-1	0	1
15	0	0	0	0	-1	-1
16	1	0	1	1	0	-1
17	0	0	0	0	0	0

The experimental runs are shuffled or randomized to reduce the potential for bias. It is to be noted that the RSM requires a very less number of experimental runs rather than the normal way of doing the experiments and hence it greatly saves time and cost. Table 5 shows the experimental and predicted values of decolorization %.

3. Results and discussion

A three-level three-factor BBD is employed for correlating decolorization % and operating variables such as effluent flow rate, ozonation time, and the number of sparger openings. For the determination of the accuracy of the reactor, ANOVA (analysis of variance) is used. ANOVA table (Table 6) reports the sum of squares, degree of freedom (DF), F -value, P -value, and model statistics. The F -value is always used with the P -value to determine the significance of p_i , p_i^2 , or $p_i p_j$ as in Eq. (1). The higher F -value corresponds to the lower P -value. The effect of the corresponding term is significant if the P -value is less than 0.05.

Values of the R^2 were determined for the developed models. The R^2 values for 100 and 50 ppm concentrations are 0.9424 and 0.7770, respectively. The adjusted R^2 (Adj.- R^2) is calculated by omitting the non-significant terms in the model. So, the Adj.- R^2 will always be less than the R^2 because of the reduction in the number of terms. As we discussed, the Adj.- R^2 has a minimal decrease, and the values are 0.8684 and 0.7255. The factor which defines how well the regression model predicts the responses for the new observation is the predicted R^2 . The difference between the predicted and adjusted R^2 values is less than 0.2 so that the model has the adequate capability to predict the response.

Table 5
Predicted and experimental values of decolorization percentage

Run order	Decolorization %			
	100 ppm concentration		50 ppm concentration	
	actual	predicted	actual	predicted
1	87.45	87.450	88.28	88.014
2	87.45	87.450	87.9	83.285
3	92.86	91.356	88.28	88.014
4	73.09	74.594	82.23	80.946
5	80.31	82.751	89.41	91.724
6	87.45	87.450	86.2	85.675
7	76.18	75.310	91.49	92.742
8	79.36	78.216	93.79	95.081
9	84.69	86.261	88.28	88.014
10	84.1	81.659	86.77	84.304
11	90.11	90.980	98.13	96.452
12	84.61	83.039	88.28	88.014
13	87.7	86.763	89.79	90.352
14	81.51	82.448	87.71	89.385
15	87.45	87.450	72.28	79.575
16	90.54	91.174	88.66	86.642
17	87.45	87.450	88.28	88.014

The coefficient of variation (C.V.) determines the degree of accuracy with which the experiments are compared. So, the higher value of C.V. indicated the low reliability of the experiment. A value below 10% indicates that the model can be considered reproducible. In the present study, the C.V. values are all below 4%, which is a good indication that our study has higher reliability of the experiments performed. Adequate precision (AP) is a factor that determines the signal to the noise ratio. AP value of greater than 4 is advantageous. AP greater than 11 is determined in our studies which indicates inadequate signal.

3.1. 100 ppm concentration

In our study, experiments for 100 ppm concentration of Congo red dye were done by changing the parameters (sparger opening, ozonation time, effluent flow rate) and calculating the value of decolorization %. The two-dimensional counterplot along with 3D response surface plots are shown in Figs. 4–6, which give insight into the relationship in the middle of the decolorization % and independent variables at one and all levels. The 3D plots give an overall idea of the response by revealing the nature of the surface as the maximum or minimum, but it may be difficult to view the levels of the variable. Therefore, 2D counterplots are represented along with 3D plots. Figs. 4–6 show the effect of two independent variables by keeping one variable constant. For example, Fig. 4 shows the response of decolorization % concerning the change in effluent flow rate and ozonation time at a constant sparger opening of 4. It is observed the decolorization % increases with an increase in both effluent flow rate and sparger opening. Likewise, these patterns are

Table 6
ANOVA table for 100 ppm concentration

Source	Sum of squares	DF	Mean squares	F-value	Prob. > F P-value
Model	416.69	9	46.30	12.73	0.0015
A – effluent flow rate	64.47	1	64.47	17.73	0.0040
B – ozonation time	199.70	1	199.70	54.92	0.0001
C – Sparger openings	91.67	1	91.67	25.21	0.0015
AB	2.13	1	2.13	0.59	0.4689
AC	7.54	1	7.54	2.07	0.1932
BC	2.81	1	2.81	0.77	0.4089
A ²	15.28	1	15.28	4.20	0.0795
B ²	11.74	1	11.74	3.23	0.1154
C ²	16.30	1	16.30	4.48	0.0720
Residual	25.45	7	3.64		
Lack of fit	25.45	3	8.48		
Pure error	0.000	4	0.000		
Cor. total	442.14	16			

Model statistics			
Std. dev.	1.91	R ²	0.9424
Mean	84.84	Adj.-R ²	0.8684
C.V.%	2.25	Pre. R ²	0.0789
PRESS	407.27	Adeq. precision	11.461

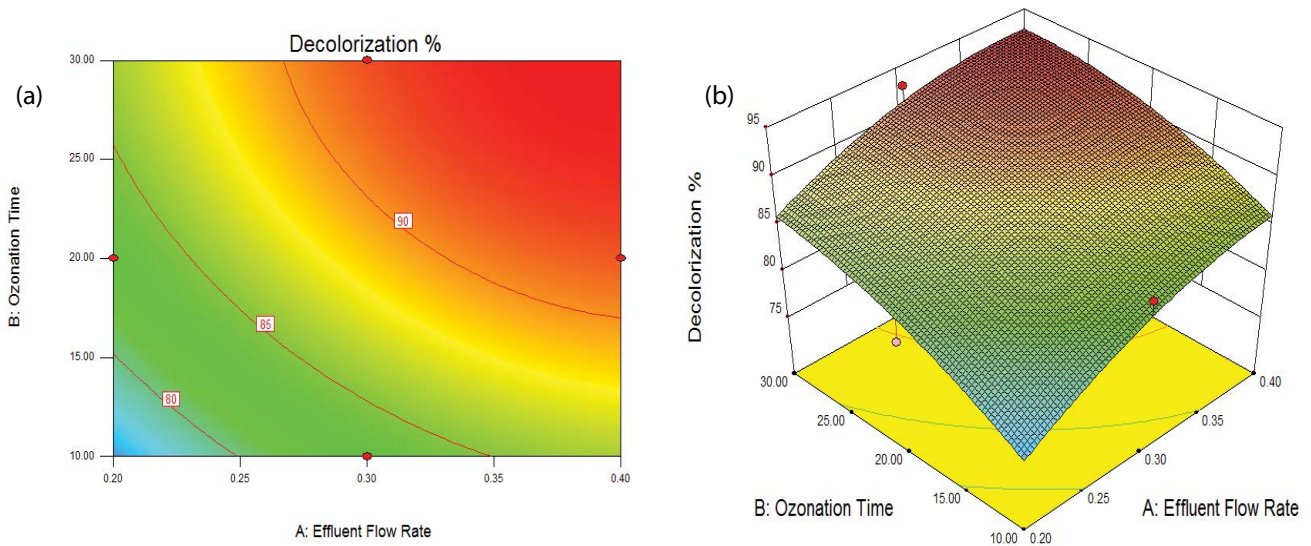


Fig. 4. Effect of effluent flow rate and ozonation time on decolorization % for the sparger opening of 4: (a) 2D contour plot and (b) 3D response surface plot.

found in Figs. 5 and 6 that with an increase in effluent flow rate, sparger opening, and ozonation time, the decolorization % also increases. The *P*-value shows the effect of linear, quadratic, and interaction terms. The effect of linear (p_1, p_2, p_3), quadratic (p_{12}, p_{22}, p_{32}), and interaction factors ($p_{1p_2}, p_{1p_3}, p_{2p_3}$) are found to significant to decolorization % according to the basis of *P*-value (<0.05).

3.2. 50 ppm concentration

The effect on decolorization % for varying independent variables was also studied for 50 ppm concentration. 2D counter plot and 3D response surface were plotted as shown in Figs. 7–9. Their corresponding ANOVA results were shown in Table 7. The influence of the independent

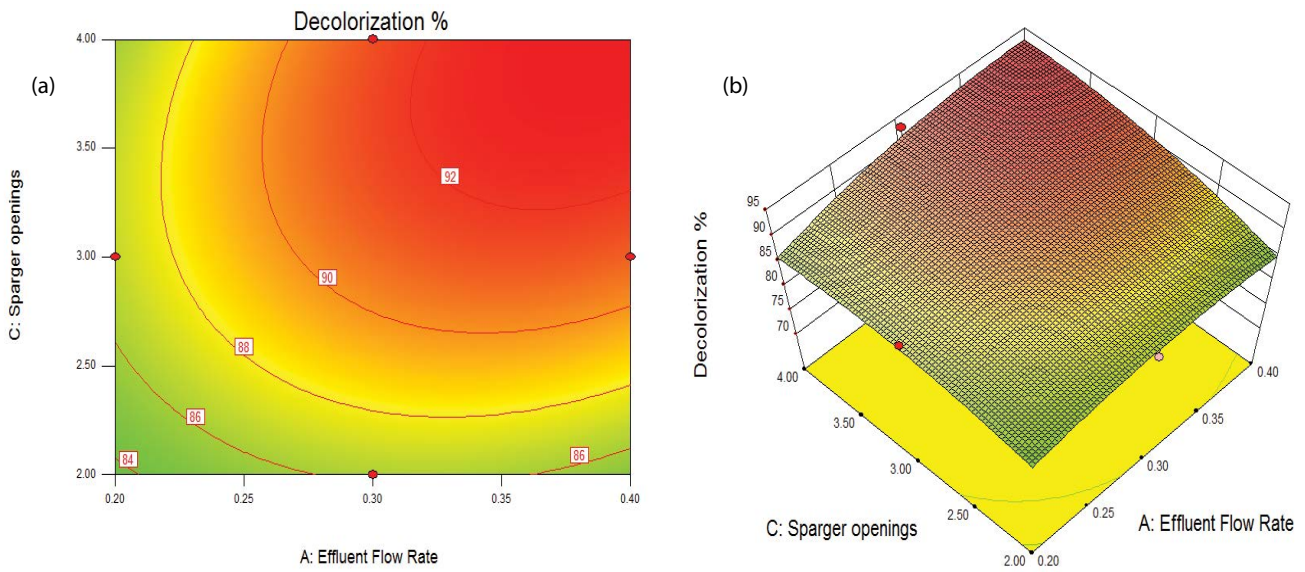


Fig. 5. Effect of effluent flow rate and sparger opening on decolorization % for the ozonation time of 30 min: (a) 2D contour plot and (b) 3D response surface plot.

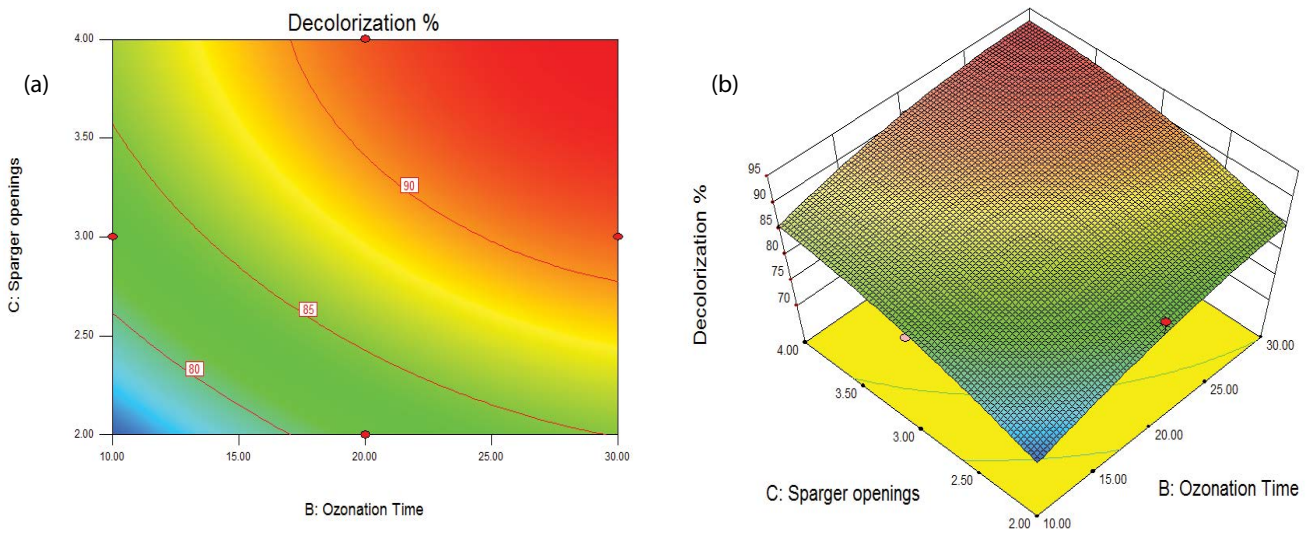


Fig. 6. Effect of ozonation time and sparger opening on decolorization % for the effluent flow rate of 0.40 L/min: (a) 2D contour plot and (b) 3D response surface plot.

variables on the decolorization % was found to be similar to the above study of 100 ppm concentration. From Figs. 7–9, with an increase in effluent flow rate, sparger opening, and ozonation time, there is an increase in decolorization %. As of Table 7, only one linear factor has a P -value less than 0.05, which indicates that these terms are notable and they are in good acceptance with observed values.

3.3. Simplified model validated by RSM

With the help of RSM, we have already found a correlation equation for each study case. The experimental decolorization percentage value was correlated successfully

with the help of RSM. This is inferred from the ANOVA which has a high coefficient of correlations. From Fig. 10 it can be seen that there is a fairly minimum deviation between the predicted and experimental values of decolorization percentage. From Table 8 it is concluded that there are 10 coefficients for Eq. (2) which seems to be longer when compared to the traditional correlation equation. And also, Eq. (2) fails to give the direct interrelationship between decolorization % and actual parameters because coded values are used instead of actual values. Due to this, a simplified correlation will be useful to determine decolorization % from the actual values rather than coded values of independent variables. From Tables 6 and 7,

Table 7
ANOVA table for 50 ppm concentration

Source	Sum of squares	DF	Mean squares	F-value	Prob. > F P-value
Model	329.27	3	109.76	15.10	0.0002
A – effluent flow rate	22.55	1	22.55	3.10	0.1017
B – ozonation time	323.31	1	232.31	31.96	<0.0001
C – Sparger openings	74.42	1	74.42	10.24	0.0070
Residual	94.50	113	7.27		
Lack of fit	94.50	9	10.50		
Pure error	0.000	4	0.000		
Cor. total	423.78	16			
Model statistics					
Std. dev.	2.70		R^2	0.7770	
Mean	88.01		Adj.- R^2	0.7255	
C.V.%	3.06		Pre. R^2	0.5340	
PRESS	197.48		Adeq. precision	12.905	

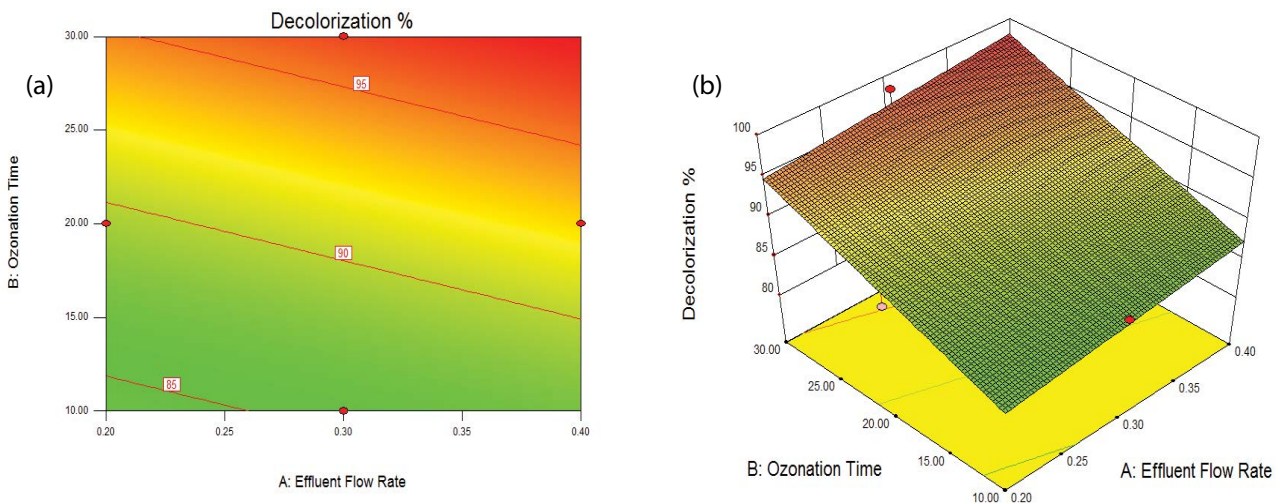


Fig. 7. Effect of effluent flow rate and ozonation time on decolorization % for the sparger opening of 4: (a) 2D contour plot and (b) 3D response surface plot.

several terms have P -values greater than 0.05 which indicates that they are insignificant for decolorization %. This simplification is done by the backward selection procedure because, in the backward selection, it starts the model with all features and then drops the least significant feature (P -value < 0.05). Therefore, these terms are excluded from Eq. (2) to get a simplified equation that correlates decolorization % and the actual variable values.

Where Y is the response, p_1 is the effluent flow rate (L/min), p_2 is the ozonation time (min), and p_3 is the sparger opening. After the simplification process, the number of coefficients (a_i) is decreased from 10 to almost 6 to 3 or there may be no simplification. This is that in those conditions all the factors play a major role in determining the decolorization %. And it is to be noted that after simplification there is only a slight change in the R^2 . Thus, the results suggest that a simplified equation can be used to find the decolorization

%. Table 8 shows the decolorization % values before and after the simplification process.

3.4. Simplified correlation validation by RSM

For the validation of the simplified equation, more experiments were carried out in RSM. The experiments were conducted in extreme conditions of BBD matrix (1, 1, 1), which are located at the vertices of the cubic model that are not comprised in the validation. And also, to confirm the vast applicability of the equation, operating conditions were chosen which are not in Tables 4 and 5 but meet the requirement of Table 3. With the help of Eq. (2) and the coefficients from Table 8, decolorization % can be determined. Table 9 shows that the experimental and predicted response is in agreement with less error percent, which is satisfactory.

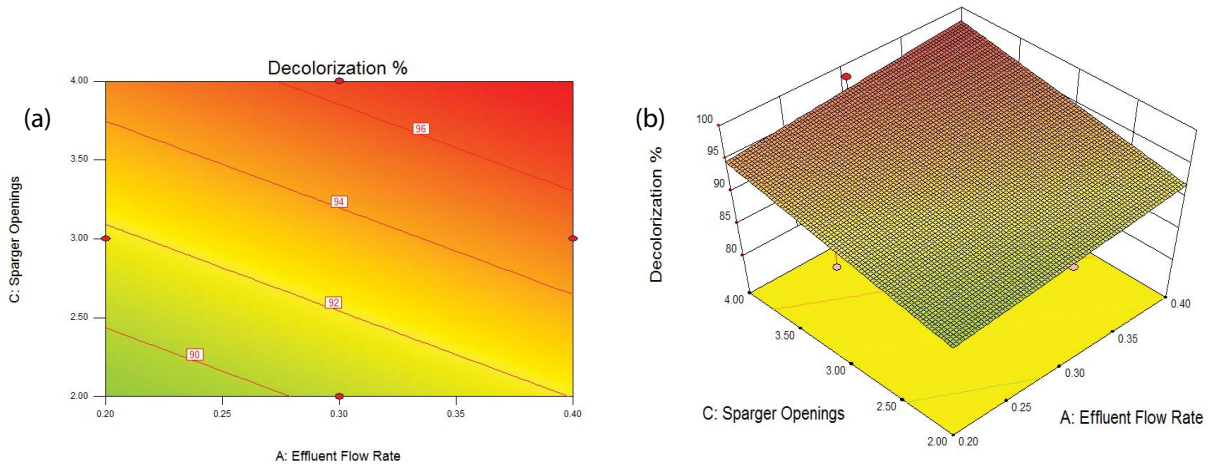


Fig. 8. Effect of effluent flow rate and sparger opening on decolorization % for the ozonation time of 30 min: (a) 2D contour plot and (b) 3D response surface plot.

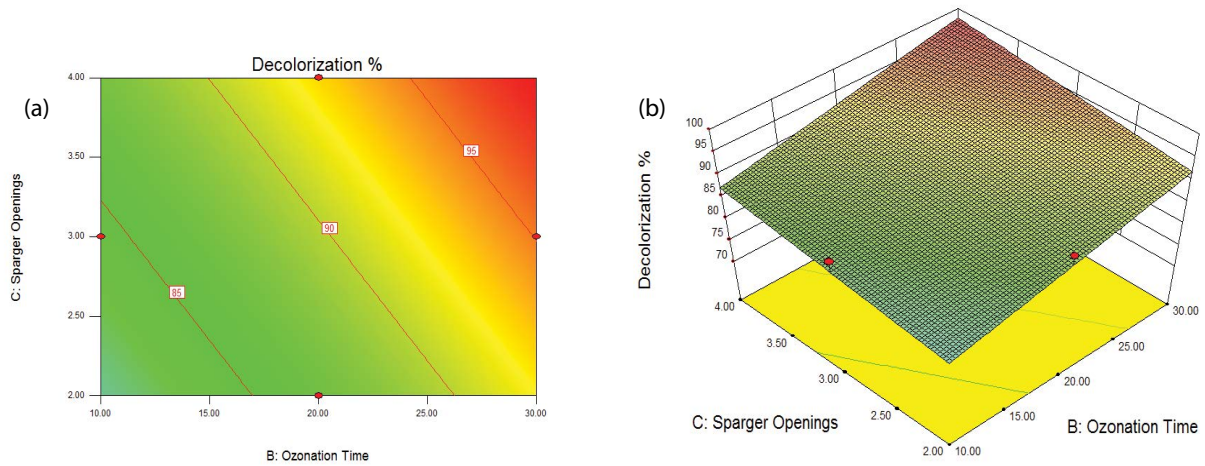


Fig. 9. Effect of ozonation time and sparger opening on decolorization % for the effluent flow rate of 0.40 L/min: (a) 2D contour plot and (b) 3D response surface plot.

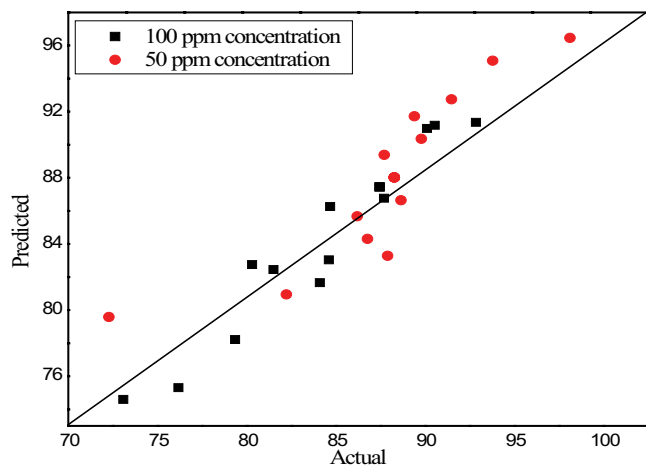


Fig. 10. Parity plot for experimental and actual values of decolorization %.

3.5. Power consumption and operating cost

Power consumption and operating cost for the down flow jet loop reactor we used in our study are shown in Table 10. A total of INR 6710 is estimated as operating cost for one month and was found to be very minimal for the maximum decolorization compared to other reactors used for similar kinds of studies as shown in Table 11.

4. Conclusion

Studies on decolorization of dye wastewater involving ozone-effluent were performed in a down flow jet loop sparged reactor. The effect of various parameters such as effluent flow rate, ozonation time, and the sparger opening on decolorization % was investigated. Maximum color removal percentage was obtained at the condition of the effluent flow rate of 0.4 L/min, ozonation time of 30 min,

Table 8
Estimated regression coefficient values of decolorization % at actual units: before and after simplification

Term	Decolorization %			
	100 ppm concentration		50 ppm concentration	
	before	after	before	after
a_0	87.45	86.75	88.28	88.01
a_1	2.84	2.84	1.68	–
a_2	5.00	5.00	5.39	5.39
a_3	3.39	3.39	3.05	3.05
a_1a_2	–0.73	–	–0.047	–
a_1a_3	1.37	–	–0.76	–
a_2a_3	–0.84	–	–1.27	–
a_1^2	–1.90	–1.99	–0.99	–
a_2^2	–1.67	–	–1.23	–
a_3^2	–1.97	–2.06	–0.33	–

and sparger openings of 4. And maximum decolorization was found up to the level of 94.56% for 100 ppm concentrated dye solution and 99.48% for 50 ppm concentrated dye solution as shown in Fig. 11. The two-phase system reveals that the decolorization percentage increases with an increase in effluent flow rate, ozonation time, and sparger openings. The conducted experiments were successfully interpreted using the RSM–BBD model, which is a handy tool for optimizing process variables.

Symbols

Y	–	Response
p_1	–	Effluent flow rate, L/min
p_2	–	Ozonation time, min
p_3	–	Number of sparger openings
N_c	–	Number of center points
n	–	Number of parameters
A_o	–	Initial absorbance value
A_t	–	Absorbance at the time

Table 9
Simplified model validation by RSM

Effluent flow rate = 0.4 L/min, ozonation time = 30 min, sparger opening = 4		
Decolorization %	100 ppm concentration	50 ppm concentration
Experimental	94.75	99.43
Predicted	93.9186	98.131
Error (%)	0.87747	1.3064
Effluent flow rate = 0.4 L/min, ozonation time = 30 min, sparger opening = 3		
Decolorization %	100 ppm concentration	50 ppm concentration
Experimental	90.11	93.76
Predicted	92.5889	95.081
Error (%)	2.7509	1.4089
Effluent flow rate = 0.4 L/min, ozonation time = 30 min, sparger opening = 2		
Decolorization %	100 ppm concentration	50 ppm concentration
Experimental	87.1	91.12
Predicted	84.1486	92.031
Error (%)	3.3885	0.9997

Table 10
Operating cost of downflow jet loop reactor

Equipment	Operating conditions	Units (W/d)	Power intensity (W/L)	Power consumption (kWh/m ³ /d)	Power consumption (kWh/m ³ /month)	Cost (one month) (In INR)
Peristaltic pump	0.2–0.4 L/min	8 W	32	16	480	1,340
Ozonator	10–30 min	15 W	60	30	900	4,370
Total cost						6,710

Note: Tamil Nadu electricity bill varies for units consumptions. For 0–500 kWh, the cost for the first 100 units is zero; for the next 100 units, the consumer shall pay 1.5 rupees per unit; for the next 300 units, the cost per unit is 3 rupees. For above 500 units, the cost for the first 100 units is zero; for the next 100 units, the consumer shall pay 3.5 rupees per unit; for the next 300 units, the cost per unit is 4.6 rupees; and for above 500, the cost per unit is 6.6 rupees.

Table 11
Decolorization percentage of various dyes performed in different reactors

Type of dye	Initial concentration of dye (mg/L)	Percentage of decolorization (%)	Reactor type	Volume of the solution (mL)	Ozonation time (min)	Reference
Methylene blue	100	88.2	Oxidation process	100	40	[22]
Methyl orange	200	89.81	Cylindrical photoreactor	20,000	60	[23]
Reactive Red 2	40	77	Hollow cylindrical glass reactor	500	30	[24]
Congo red	100	96	Down flow jet loop reactor	250	30	This study

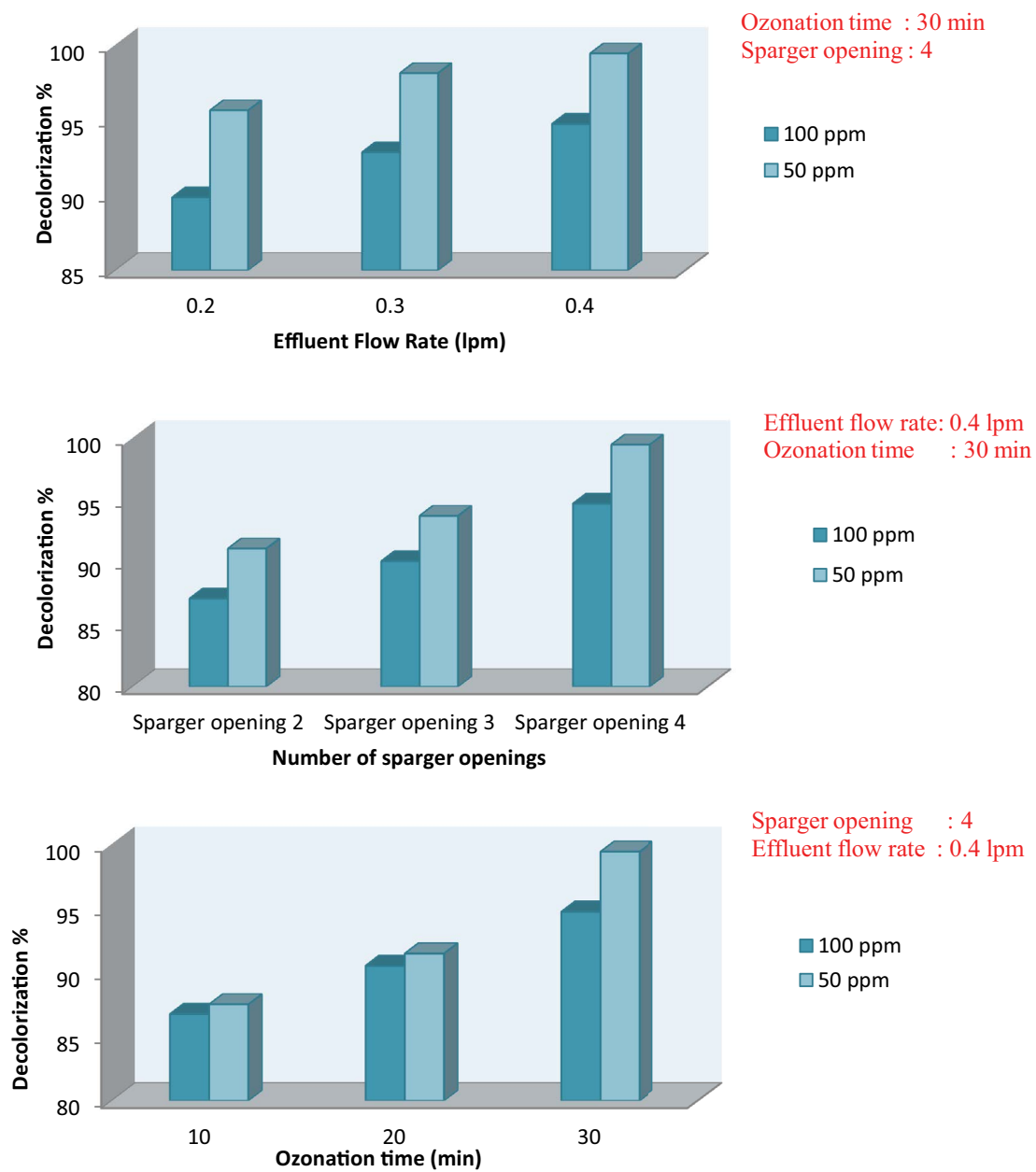


Fig. 11. Pareto chart.

References

- [1] D.A. Yaseen, M. Scholz, Textile dye wastewater characteristics and constituents of synthetic effluents: a critical review, *Int. J. Environ. Sci. Technol.*, 16 (2019) 1193–1226.
- [2] A. Seidmohammadi, Gh. Asgari, A. Dargahi, M. Leili, Y. Vaziri, B. Hayati, A.A. Shekarchi, A. Mobarakian, A. Bagheri, S.B. Nazari Khanghah, A. Keshavarzpour, A comparative study for the removal of Methylene blue dye from aqueous solution by novel activated carbon based adsorbents, *Prog. Color Colorants Coat.*, 12 (2019) 133–144.
- [3] M.R. Samarghandi, A. Dargahi, A. Shabanloo, H. Zolghadr Nasab, Y. Vaziri, A. Ansari, Electrochemical degradation of Methylene blue dye using a graphite doped PbO₂ anode: optimization of operational parameters, degradation pathway and improving the biodegradability of textile wastewater, *Arabian J. Chem.*, 13 (2020) 6847–6864.
- [4] M.R. Samarghandi, A. Dargahi, H. Zolghadr Nasab, E. Ghahramani, S. Salehi, Degradation of azo dye Acid Red 14 (AR14) from aqueous solution using H₂O₂/nZVI and S₂O₈²⁻/nZVI processes in the presence of UV irradiation, *Water Environ. Res.*, 92 (2020) 1173–1183.
- [5] B. Lellis, C.Z. Fávoro-Polonio, J. Alencar Pamphile, J.C. Polonio, Effects of textile dyes on health and the environment and bioremediation potential of living organisms, *Biotechnol. Res. Innovation*, 3 (2019) 275–290.
- [6] K. Hasani, M. Moradi, S.A. Mokhtari, Hadi sadeghi, A. Dargahi, M. Vosoughi, Degradation of basic violet 16 dye by electro-activated persulfate process from aqueous solutions and toxicity assessment using microorganisms: determination of by-products, reaction kinetic and optimization using Box–Behnken design, *Int. J. Chem. Reactor Eng.*, 19 (2021) 261–275.
- [7] Y.-C. Hsu, J.-T. Chen, H.-C. Yang, J.-H. Chen, Decolorization of dyes using ozone in a gas-induced reactor, *Am. Inst. Chem. Eng. J.*, 47 (2001) 169–175.
- [8] A.H. Konsowa, Decolorization of wastewater containing direct dye by ozonation in a batch bubble column reactor, *Desalination*, 158 (2003) 233–240.
- [9] R.Y. Peng, H.-J. Fan, Ozonolytic kinetic order of dye decoloration in aqueous solution, *Dyes Pigm.*, 67 (2005) 153–159.
- [10] E. Oguz, B. Keskinler, Removal of color and COD from synthetic textile wastewater using O₃, PAC, H₂O₂ and HCO₃⁻, *J. Hazard. Mater.*, 151 (2008) 753–760.
- [11] O.J. Hao, H. Kim, P.-C. Chiang, Decolorization of wastewater, *Crit. Rev. Env. Sci. Technol.*, 30 (2000) 449–505.
- [12] A. Helble, W. Schlager, P.-A. Liechti, R. Jenny, C.H. Möbiust, Advanced effluent treatment in the pulp and paper industry with a combined process of ozonation and fixed bed biofilm reactors, *Water Sci. Technol.*, 40 (1999) 343–350.
- [13] M.F. Sevimli, C. Kinaci, Decolorization of textile wastewater by ozonation and Fenton's process, *Water Sci. Technol.*, 45 (2002) 279–286.
- [14] H. Brauer, D. Saucker, Biological wastewater treatment in high-efficiency reactor, *Ger. Chem. Eng.*, 2 (1979) 77–86.
- [15] U. Wachsmann, N. Rabiger, A. Vogelpohl, The compact reactor – a newly developed loop reactor with high mass transfer performance, *Ger. Chem. Eng.*, 7 (1984) 39–44.
- [16] M. Velan, T.K. Ramanujam, Hydrodynamics in down flow jet loop reactor, *The Can. J. Chem. Eng.*, 69 (1991) 1257–1261.
- [17] K. Hasani, A. Peyghami, A. Moharrami, M. Vosoughi, A. Dargahi, The efficacy of sono-electro-Fenton process for removal of cefixime antibiotic from aqueous solutions by response surface methodology (RSM) and evaluation of toxicity of effluent by microorganisms, *Arabian J. Chem.*, 13 (2020) 6122–6139.
- [18] M. Heidari, M. Vosoughi, H. Sadeghi, A. Dargahi, S.A. Mokhtari, Degradation of diazinon from aqueous solutions by electro-Fenton process: effect of operating parameters, intermediate identification, degradation pathway, and optimization using response surface methodology (RSM), *Sep. Sci. Technol.*, 56 (2021) 2287–2299.
- [19] A. Almasi, M. Mahmoudi, M. Mohammadi, A. Dargahi, H. Biglari, Optimizing biological treatment of petroleum industry wastewater in a facultative stabilization pond for simultaneous removal of carbon and phenol, *Toxic Rev.*, 40 (2021) 189–197.
- [20] S. Afshin, Y. Rashtbari, M. Vosough, A. Dargahi, M. Fazlzadeh, A. Behzad, M. Yousefi, Application of Box–Behnken design for optimizing parameters of hexavalent chromium removal from aqueous solutions using Fe₃O₄ loaded on activated carbon prepared from alga: kinetics and equilibrium study, *J. Water Process Eng.*, 42 (2021) 102113, doi: 10.1016/j.jwpe.2021.102113.
- [21] S. Alizadeh, H. Sadeghi, M. Vosoughi, A. Dargahi, S. Ahmad Mokhtari, Removal of humic acid from aqueous media using sono-persulphate process: optimization and modelling with response surface methodology (RSM), *Int. J. Environ. Anal. Chem.*, (2020) 1772777, doi: 10.1080/03067319.2020.1772777.
- [22] J. Zhang, K.-H. Lee, L. Cui, T.-S. Jeong, Degradation of Methylene blue in aqueous solution by ozone-based processes, *J. Ind. Eng. Chem.*, 15 (2009) 185–189.
- [23] X.-f. Lü, H.-r. Ma, Q. Zhang, K. Du, Degradation of Methyl orange by UV, O₃ and UV/O₃ systems: analysis of the degradation effects and mineralization mechanism, *Res. Chem. Intermed.*, 39 (2013) 4189–4203.
- [24] C.-H. Wu, H.-Y. Ng, Degradation of C.I. Reactive Red 2 (RR2) using ozone-based systems: comparisons of decolorization efficiency and power consumption, *J. Hazard. Mater.*, 152 (2008) 120–127.